

Supplementary Information

Efficiency enhancement of solid-state PbS quantum dot-sensitized solar cells with Al_2O_3 barrier layer

Thomas P. Brennan,^{a†} Orlando Trejo,^{b†} Katherine E. Roelofs,^{a,c} John Xu,^b Fritz B. Prinz,^b and Stacey F. Bent^a

^a Department of Chemical Engineering, Stanford University, Stanford, CA 94305, USA

^b Department of Mechanical Engineering, Stanford University, Stanford, CA 94305, USA

^c Department of Materials Science and Engineering, Stanford University, Stanford, CA 94305, USA

† These authors contributed equally to this work.

Schematics of Barrier Layer Configurations

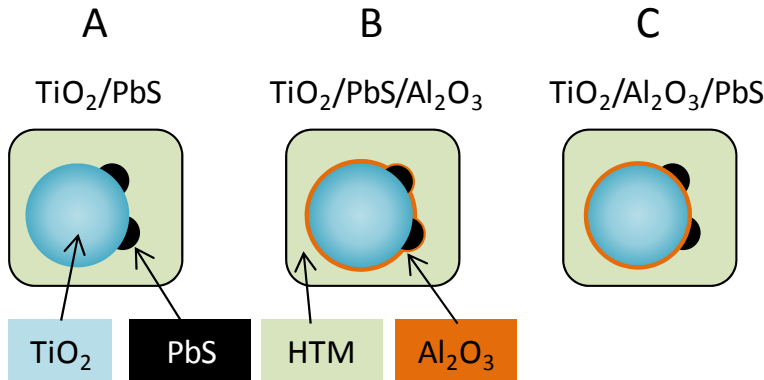


Fig. S1: Schematics of the three configurations studied (not to scale). A: control devices with PbS quantum dots grown on TiO₂ nanoparticles, surrounded by the spiro-OMeTAD hole transport material (HTM). B: Al₂O₃ deposited after growth of quantum dots. In this configuration the Al₂O₃ barrier layer is expected to slow recombination involving electrons in TiO₂ and holes in the HTM. C: Al₂O₃ deposited prior to quantum dot growth. In this configuration the Al₂O₃ barrier layer is expected to slow recombination involving electrons in TiO₂ and holes in both the HTM and oxidized quantum dots. Configuration C yielded the highest device efficiencies.

Experimental Details & Additional Data

Fabrication of Nanostructured TiO₂ Substrates

As described elsewhere,¹ fluorine-doped tin oxide (FTO)-coated glass (Pilkington, 15 Ω/□) was etched using 4 M HCl and Zn powder in order to create the desired device pattern. A compact layer of TiO₂ ~50 nm thick (to prevent contact between the FTO and the hole-transport material (HTM)) was deposited on the substrates at 450 °C by spray pyrolysis of titanium diisopropoxide bis(acetylacetone) (Aldrich) in ethanol (1:9 v/v) using air as the carrier gas. Roughly 2 μm-thick nanoporous TiO₂ films were made by doctor-blading a 1:1 (w/w) ratio of terpineol and a commercial paste (Dyesol 18NR-T) atop the compact TiO₂ layer followed by an anneal at 450 °C. The substrates were then left overnight in a bath of aqueous 0.02 M TiCl₄ and subsequently annealed again at 450 °C for thirty minutes.

Atomic Layer Deposition of PbS and Al₂O₃

The PbS quantum dots were deposited by using a low number of ALD cycles on nanoporous TiO₂ substrates. Bis(2,2,6,6-tetramethyl-3,5-heptanedionato)lead(II) (Pb(tmhd)₂) (Strem Chemicals, Inc.), sublimated at 140 °C, and 3.5% H₂S in N₂ were the deposition reagents. At a temperature of 160 °C, the reactions took place in a customized ALD station that is H₂S compatible.² Pulse/purge times of 0.5/45 s for Pb(tmhd)₂ and 0.1/40 s for H₂S were used. In the same reactor and conditions, Al₂O₃ was deposited at 160 °C using trimethylaluminum (TMA) (Aldrich) and DI water as the deposition reagents. Pulse/purge times of 0.1/40 s were used for both TMA and H₂O. Promptly after deposition, the samples were stored in an inert environment awaiting further processing and characterization.

Auger electron spectroscopy (AES) was used to verify growth of the quantum dots throughout the depth of a ~5 μm thick nanoporous TiO₂ film made in the same fashion as the ~2 μm thick TiO₂ films used in devices. The results of an AES linescan of a nanoporous TiO₂ film on a silicon substrate are shown in Fig. S2 both as the raw signal intensity and the corresponding atomic concentrations. Despite the fact that the ALD process was not optimized for films as thick as 5 μm, the data indicate

growth of PbS throughout this nanoporous TiO₂ layer, which is much thicker than that used in devices. The signal intensity of sulphur is independent of depth in the substrate, although there is some dropoff in the lead signal away from the surface which could be due to superior infiltration of the smaller sulphur precursor.

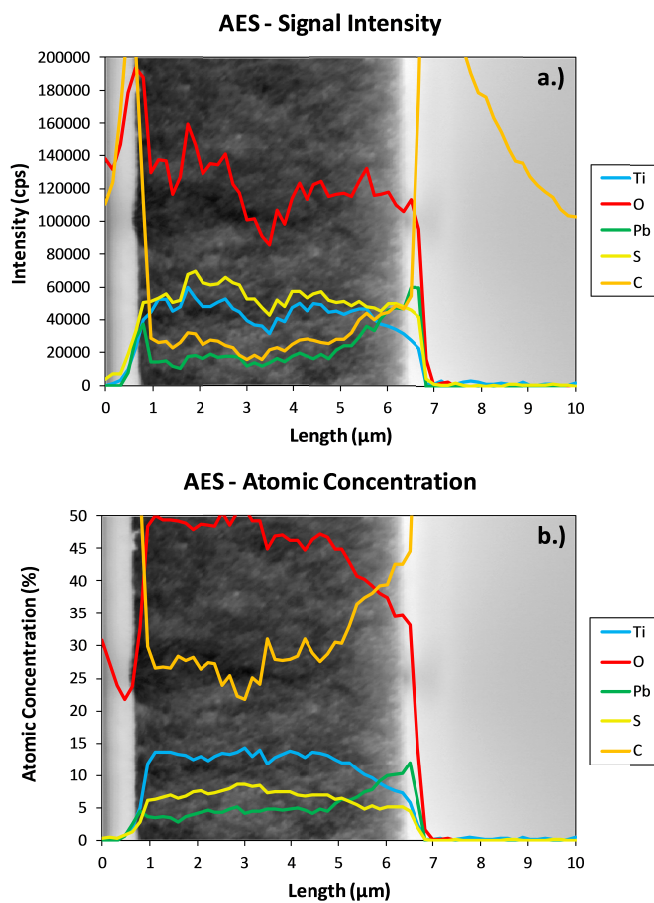


Fig. S2 Auger electron spectroscopy linescan of 10 ALD cycles of PbS grown on a nanoporous TiO₂ substrate with data reported in terms of signal intensity, a), and atomic concentration, b). The linescan was performed at the midpoint of the SEM image, *i.e.* the 100000 counts per second (CPS) line in a), and the 25% line in b). The nanoporous TiO₂ layer, approximately 5 μm thick, was deposited atop a silicon substrate which is at the far left of the SEM image, meaning that the top of the nanoporous TiO₂ film is at approximately the 6 μm mark.

QDSSC Device Fabrication

Spiro-OMeTAD ($(2,2',7,7'\text{-tetrakis-(}N,N\text{-di-}p\text{-methoxyphenylamine)\text{-}9,9'\text{-spirobifluorene}}$) (Lumtec) was dissolved in chlorobenzene at a concentration of 225 mL^{-1} . *Tert*-butylpyridine was added to the solution at the ratio of $1:10.3 \text{ }\mu\text{L:mg}$ of spiro-OMeTAD, and lithium bis-(trifluoromethylsulfonyl)imide salt (170 mg mL^{-1} in acetonitrile) was added at the ratio of $1:4.8 \text{ }\mu\text{L:mg}$ of spiro-OMeTAD. The resultant solution was deposited onto QD-coated TiO_2 substrates ($\sim 30 \text{ }\mu\text{L per } 3 \text{ cm}^2$ substrates) and then spin-coated for 30 s at 2000 RPM. 200 nm-thick silver electrodes were then evaporated onto the substrates under vacuum at 10^{-6} torr yielding device areas $\sim 9\text{-}10 \text{ mm}^2$.

Device Testing

Solar cell performance was measured as described elsewhere.¹ Current-voltage ($J\text{-}V$) curves were obtained using a Xe lamp AM 1.5 solar simulator calibrated to 1 sun. Devices were light-soaked until maximum efficiencies were obtained (~ 30 minutes). Recombination lifetimes were obtained *via* transient photovoltage experiments.^{3, 4} Devices were biased at 1 sun using a white LED array. A Keithley 2400 SourceMeter was used to keep the device current constant at a value corresponding to a given photovoltage (the photovoltage was swept in 0.05 V increments). A white LED (~ 0.05 sun) was then pulsed (50 ms square-wave) at the samples, yielding a transient increase and subsequent decrease in the device photovoltage. Recombination lifetimes were obtained by fitting the exponential decay of the photovoltage. Incident photon-to-current efficiency (IPCE; also known as external quantum efficiency, or EQE) measurements were taken at short circuit using monochromated white light from a 100 W tungsten lamp, which was focused through a monochromator. The monochromated illumination, chopped at 40 Hz, was superimposed on top of a continuous-wave white light illumination (~ 1 sun) from a white LED array incident on the device. The photocurrent action spectrum of the device was acquired through a lock-in amplifier and IPCE was calculated by referencing the device current to a NIST traceable

calibration photodiode. While we have not performed rigorous long-term device stability studies, we note that device performance (and behavior, for example, in recombination measurements) is reproducible over several-day time intervals.

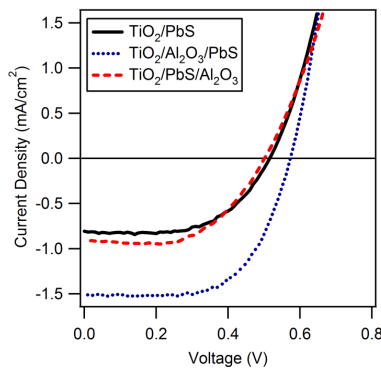


Fig. S3 Light current-voltage (J - V) curves for typical devices of the four configurations studied. The large enhancement in the $\text{TiO}_2/\text{Al}_2\text{O}_3/\text{PbS}$ configuration versus the other three configurations is apparent, especially in the short-circuit current, J_{SC} , but also in the open-circuit voltage, V_{OC} .

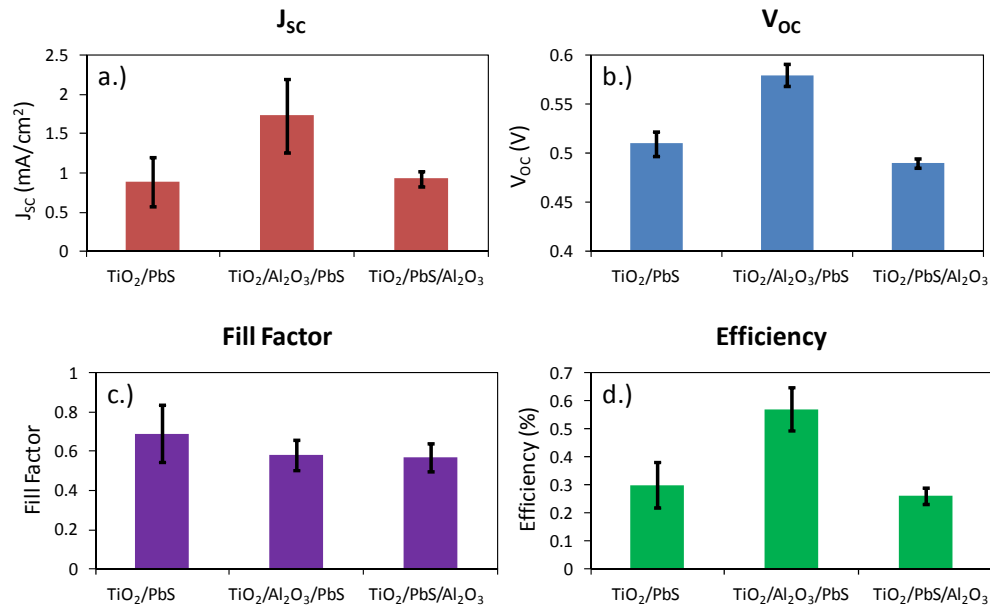


Fig. S4 – Average device data for the PbS QDSSCs with and without Al_2O_3 barrier layers. Values were calculated by averaging the top two (of four) devices on each of four separate substrates for

each configuration; therefore the values represent the average of eight different devices. Error bars indicate standard deviation of device parameters.

Characterization *via* Transmission Electron Microscopy (TEM) and UV-Vis Spectroscopy

Plain-view TEM micrographs of the samples were taken using a FEI Tecnai G2 F20-X-TWIN at an accelerating voltage of 200 kV. Before TEM characterization, the PbS QD/nanoporous TiO₂ composite films were scratched off from the glass substrates using a sterile razor. Afterwards, the residue was sonicated in 1 mL of ethanol for 5 mins. A fresh ultrathin carbon on copper TEM grid (Ted Pella, Inc.) was introduced into the solution to extract PbS QD/nanoporous TiO₂ clusters.

Table S1. Average atomic concentrations measured using TEM-EDS. The atomic shells used for each element are denoted inside parentheses.

Atomic Species (shell)	PbS x 10	Al ₂ O ₃ x 1 + PbS x 10
C (K)	54.3	50.0
O (K)	15.3	24.4
Al (K)	-	0.8
S (K)	1.9	0.3
Ti (K)	8.1	10.9
Cu (K)	17.8	13.0
Pb (L)	2.6	0.6

Also in the TEM, Energy-dispersive spectroscopy (EDS) was performed on the X-rays emitted by the samples of interest. EDS helped identify the main atomic species present. Table S1 summarizes the average atomic concentrations of the samples with PbS QDs on nanoporous TiO₂ with and without the Al₂O₃ barrier layer. No samples with spiro-OMeTAD were analyzed using TEM-EDS. The X-ray signal is

dominated by the carbon and copper peaks from the TEM grid. The comparable atomic concentrations of Pb and S strongly suggest the existence of PbS in the samples.

UV-Vis measurements were taken using two different methods. In the data shown below in Fig. S5, spectra were obtained using a PerkinElmer Lambda 1050 UV/VIS/NIR Spectrometer. The samples were measured as deposited after the ALD step (*i.e.* lacking both spiro-OMeTAD and silver electrodes). The spectra shown in Fig. 2a in the manuscript, on the other hand, were collected from complete devices. These measurements, reported in terms of spectral absorptance, were collected using the same tungsten lamp and monochromator as the IPCE measurements and were measured using an integrating sphere with an attached silicon photodiode.

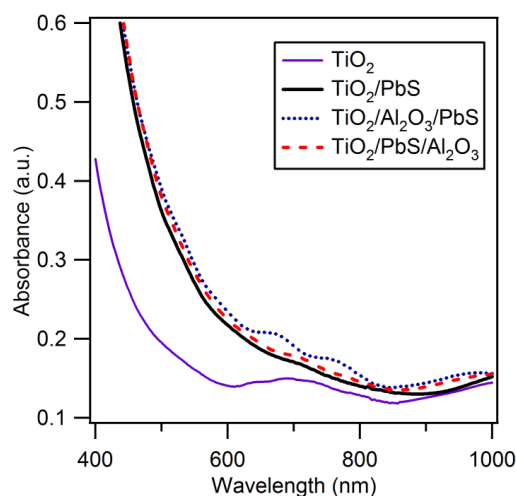


Fig. S5 UV-Vis absorbance spectra taken in transmission mode of nanoporous TiO_2 substrates on FTO coated with PbS QDs in the three different configurations studied. A TiO_2 control is also shown. No significant changes were observed when a single ALD cycle of Al_2O_3 preceded PbS deposition indicating that it did not lead to enhanced PbS nucleation. In all three configurations containing PbS QDs, the absorption onset occurs near 800 nm indicating a band gap for the largest QDs ~1.6 eV.

References

1. T. Leijtens, I. K. Ding, T. Giovenzana, J. T. Bloking, M. D. McGehee and A. Sellinger, *ACS Nano*, 2012, **6**, 1455-1462.

2. N. P. Dasgupta, J. F. Mack, M. C. Langston, A. Bousetta and F. B. Prinz, *Review of Scientific Instruments*, 2010, **81**, 044102-044106.
3. B. C. O'Regan and F. Lenzmann, *The Journal of Physical Chemistry B*, 2004, **108**, 4342-4350.
4. B. C. O'Regan, J. R. Durrant, P. M. Sommeling and N. J. Bakker, *The Journal of Physical Chemistry C*, 2007, **111**, 14001-14010.